Biol. Cell (2014) **106,** 1–15 DOI: 10.1111/boc.201300075

Research article

Secretory Leukocyte Protease Inhibitor (SLPI) expression downregulates E-cadherin, induces β-catenin re-localisation and triggers apoptosis-related events in breast cancer cells

Marina Rosso*[1], Lara Lapyckyj*[1], Nicolás Amiano†, María José Besso*, Mercedes Sánchez†, Eduardo Chuluyan† and Mónica Hebe Vazquez-Levin*[2]

*Instituto de Biología & Medicina Experimental (IBYME), National Research Council of Argentina (CONICET), Vuelta de Obligado 2490, Buenos Aires C1428ADN, Argentina and †3a. Cátedra de Farmacología, Facultad de Medicina, Universidad de Buenos Aires, 9° Piso, Paraguay 2155, Buenos Aires C1121ABG, Argentina

Background Information. Epithelial cadherin (E-cadherin) is involved in cell–cell adhesion through its extracellular domain, whereas the intracellular domain interacts with adaptor proteins, i.e. β-catenin, links E-cadherin to the actin cytoskeleton and participates in signal transduction events. E-cadherin protects mammary epithelial cells from apoptosis and its loss during tumour progression has been documented. Secretory Leukocyte Protease Inhibitor (SLPI) has anti- and pro-tumourigenic activities but its role in breast cancer has not been fully elucidated. Notwithstanding its relevance, how SLPI affects E-cadherin in breast cancer is still unknown. This study evaluated the effect of SLPI upon E-cadherin/β-catenin expression and apoptosis-related markers in murine (F3II) and human (MCF-7) breast tumour cells either treated with exogenous recombinant human SLPI (rhSLPI) or stably transfected with a plasmid encoding its sequence.

Results. Addition of rhSLPI to F3II cells caused a decrease ($P < 0.05$) in E-cadherin transcript and protein levels. Similar results were observed in SLPI-stable F3II transfectants (2C1), and treatment of 2C1 cells with a siRNA toward SLPI restored E-cadherin to control levels. SLPI-expressing cells showed disruption of E-cadherin/β-catenin complex and increased ($P < 0.05$) percentage of cells depicting nuclear β-catenin localisation. Associated to these changes, 2C1 cells showed increased Bax/Bcl-2 ratio and p21 protein levels, decreased c-Myc protein levels and decreased Cyclin D1 and Claudin-1 transcript levels. No differences in N- and P-cadherin were observed between SLPI-transfected cells and controls. Addition of rhSLPI to MCF-7 cells or stable transfection with SLPI caused a decrease ($P < 0.05$) in E-cadherin expression (transcript/protein) and its redistribution to the cytoplasm, as well as β-catenin re-localisation to the cell nucleus.

Conclusions. Expression of SLPI was associated to a decrease in E-cadherin expression and re-localisation of E-cadherin to the cell cytoplasm and β-catenin to the cell cytoplasm and nucleus, and had pro-apoptotic and cell cycle-arrest effects.

[1]These authors equally contributed to this work.
[2]To whom correspondence should be addressed (email: mhvazl@gmail.com)
The studies here described have been recently presented by M.R. at the 18th International Meeting of the European Society of Gynaecological Oncology (ESGO; Liverpool, UK; 19–22 October 2013).
Key words: Apoptosis, β-catenin, Cancer, Cell adhesion, Epithelial cadherin, SLPI.
Abbreviations used: CM, conditioned media; E-cadherin, epithelial cadherin; GAPDH, glyceraldehyde 3-phosphate dehydrogenase; rhSLPI, recombinant human SLPI; siSLPI, siRNA for hSLPI; SLPI, Secretory leukocyte protease inhibitor.

Introduction

Cell–cell adhesion is relevant for the maintenance of tissue homeostasis, since it is involved in the assembly of the epithelial structure, as well as in regulating cell fate towards differentiation, death and/or survival. Cell–cell interactions control cell survival mostly via the classical cadherins, a superfamily of mainly transmembrane glycoproteins that mediate Ca^{2+}-dependent cell–cell adhesion. Disruption of cadherin-mediated epithelial cell adhesion leads to increased apoptosis and decreased cell survival. In particular, expression of epithelial cadherin (E-cadherin) has been reported to protect cells from apoptosis in several models (Day et al., 1999; Wang et al., 2009).

E-cadherin is the founder member of the cadherin superfamily (Takeichi, 1977; Angst et al., 2001). The E-cadherin mature glycoprotein is a 120 kDa polypeptide organised in an extracellular domain that mediates cell–cell adhesion, a transmembrane domain and a highly conserved cytoplasmic domain that links E-cadherin to filamentous actin (F-actin) through adaptor molecules (β-catenin and others) for strengthening cellular adhesion, and it is also involved in protein trafficking and cell signalling (van Roy and Berx, 2008).

In several cancers, defects in E-cadherin expression have been associated to transcriptional repression and to post-translational modifications of the mature protein. Concomitant to the decrease in E-cadherin, β-catenin dissociates from the adhesion protein and re-localises to the cytoplasm and eventually to the nucleus, where it may act as a co-transcription factor. In addition, expression of other classical cadherins, such as Neural (N-cadherin) and Placental (P-cadherin) cadherin, has been reported in association to a more invasive cell phenotype (van Roy and Berx, 2008). During breast tumour progression, E-cadherin-mediated cell–cell adhesion is altered, resulting in activation of several signalling pathways (Birchmeier et al., 1995; Conacci-Sorrell et al., 2002).

The extracellular microenvironment has been widely recognised to influence tumour behaviour. In particular, secreted proteases can activate growth factors and remodel the extracellular matrix and protease inhibitors present anti-tumour activity since they abolish protease enzymatic activity. The expression of the Secretory Leukocyte Protease Inhibitor (SLPI) (also named antileukoproteinase-1) and its role in tumour progression has not been fully established. Specifically regarding SLPI in breast cancer, both decreased and increased expression levels of SLPI have been related to tumour progression and regression (Hu et al., 2004; Kluger et al., 2004). A retrospective microarray study revealed an association of increased SLPI expression and both disease-free and overall patient survival (Cimino et al., 2008). In agreement with these findings, two recent reports from members of this team described the ability of SLPI to restrain tumour growth and increase animal survival by inducing some apoptosis-related changes (Amiano et al., 2011, 2013).

Until the present time, no studies have reported whether changes in SLPI in tumour cells affect expression and localisation of members of the adherent complex, in particular E-cadherin and β-catenin. The aim of this work was to evaluate the effect of SLPI on the expression of E-cadherin and other members of the adherent complex (β-catenin and F-actin), as well as on N-cadherin, P-cadherin, apoptosis- and cell cycle arrest-related markers in a murine and a human *in vitro* breast cancer model.

Results

SLPI modulation of E-cadherin expression in a murine breast cancer cell model

To characterise the effect of SLPI upon proteins from the adherent complex, a set of studies were done using a murine mammary cancer model. The F3II mammary carcinoma cell line derived from BALB/c mice was selected for these experiments; characteristics of this cell line are presented in *Materials and Methods*. Treatment of F3II cells with 0.4 and 4 μg/ml recombinant human SLPI (rhSLPI) resulted in a decrease ($P < 0.05$) of E-cadherin protein levels, with a $79 \pm 2\%$ (mean ± SEM) reduction when SLPI was added at the highest concentration (Figure 1A).

To further characterise the effect of SLPI expression upon E-cadherin, studies were carried out in 2C1 cells, SLPI-stable transfectants of F3II cells; the F3II-pcDNA (pcDNA3-stable transfectants of F3II) cells served as control (Amiano et al., 2011). In all cultures, the expression of SLPI mRNA in the 2C1 cells was verified by standard RT-PCR (Figure 1B,

Figure 1 | Effect of SLPI treatment in F3II murine breast cancer cells upon E-cadherin expression

(**A**) Western immunoblotting (left panel) and densitometric analysis (right panel) of 120 kDa full-length E-cadherin protein levels in protein extracts from F3II mouse breast tumour cells incubated with rhSLPI (ns: not significant; $^*P < 0.05$). (**B**) Standard RT-PCR analysis of SLPI mRNA expression in F3II control (F3II-pcDNA3) and SLPI (2C1) transfected cells (left panel). SLPI concentration in 2C1 and F3II-pcDNA3 cell culture supernatants was estimated by means of an ELISA sandwich (right panel; $^*P < 0.05$). (**C**) Quantitative analysis of E-cadherin mRNA expression levels in F3II-pcDNA3 and 2C1 cells (qPCR; $^*P < 0.05$). (**D**) Western immunoblotting (left panel) and densitometric analysis (right panel) of 120 kDa full-length E-cadherin protein in F3II-pcDNA3 and 2C1 total cell lysates ($^*P < 0.05$). Actin is included as protein loading control. (**E**) Effect of SLPI-silencing (siSLPI; control: siCTRL) in 2C1 cells upon E-cadherin mRNA expression levels (left panel; $^*P < 0.05$); SLPI concentration in 2C1 siSLPI and 2C1 siCTRL cell culture supernatants assessed by means of an ELISA sandwich (right panel; $^*P < 0.05$).

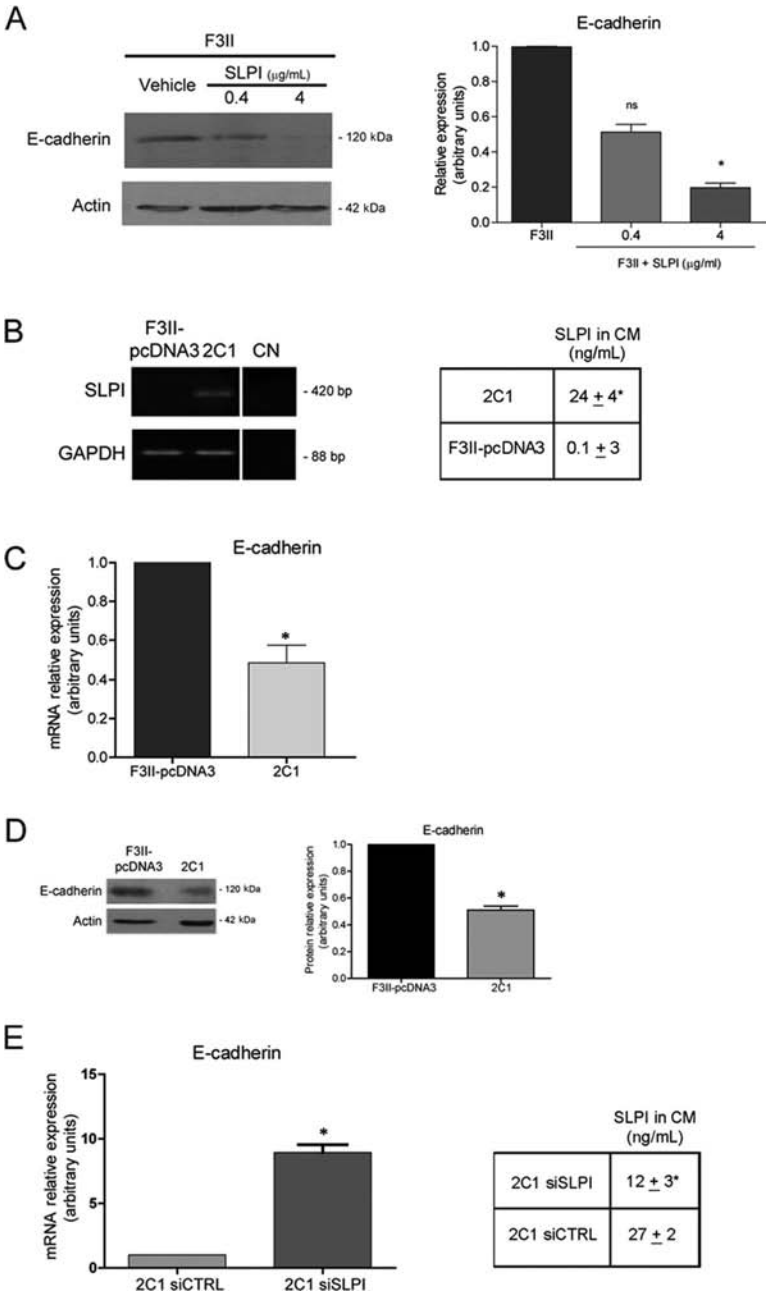

left panel). In addition, the SLPI protein present in the conditioned media (CM) of 2C1 and F3II-pcDNA3 control cells was quantitated in all cultures by means of a sensitive and specific ELISA, finding higher ($P < 0.001$) levels of SLPI in the 2C1 transfectants compared with controls (Figure 1B, right panel).

A quantitative analysis, done by means of real time PCR, revealed lower ($P < 0.05$) expression levels of E-cadherin mRNA in 2C1 cells compared with F3II-pcDNA3 control cells (Figure 1C). In agreement with these findings, E-cadherin protein analysis done by Western immunoblotting revealed a lower ($P < 0.05$) signal for the 120 kDa full-length adhesion protein in the SLPI-expressing transfectants when compared with control F3II-pcDNA3 cells (Figure 1D, left panel); a 51 $\pm$ 3% reduction of E-cadherin was estimated by densitometric analysis (Figure 1D, right panel).

The results obtained with the 2C1 cells would indicate that expression of SLPI results in downregulation of E-cadherin. To confirm this association, 2C1 cells were incubated with a specific siRNA for hSLPI (siSLPI) or with a scramble siRNA (siCTRL), and E-cadherin mRNA levels were assessed by qPCR. The effectiveness of the siRNA treatment on SLPI expression was confirmed by decreased ($P < 0.05$) levels of the SLPI secreted protein present in the CM by ELISA (Figure 1E, right panel). E-cadherin mRNA expression levels were higher ($P < 0.05$) in 2C1 siSLPI cells compared with the siCTRL control condition (Figure 1E, left panel). Interestingly, E-cadherin levels in 2C1 siSLPI cells were comparable to those found in F3II-pcDNA3 cells (E-cadherin relative expression in 2C1 siSLPI = 0.9 $\pm$ 0.05, F3II-pcDNA3 = 1).

SLPI effect on downregulation of E-cadherin expression and EMT-related mechanisms

To analyse the molecular basis of the decrease in E-cadherin protein and transcript levels observed in murine breast cancer cells expressing SLPI, a set of experiments were done, as follows.

The reduction in E-cadherin expression associated to the SLPI expression could be related to activity of metalloproteinases that degrade the adhesion molecule, rendering an intracellular membrane associated CTF1 fragment of 38 kDa and a 86 kDa soluble fragment known as the E-cadherin ectodomain (van Roy and Berx, 2008). Presence of E-cadherin processing fragments was evaluated by Western immunoblotting of total cellular extracts and CM proteins from 2C1 and F3II-pcDNA3 cells. Whereas a signal for the CTF1 fragment was found among F3II-pcDNA3 proteins, it was not detected in protein profiles from 2C1 cell extracts; in agreement with these results, the E-cadherin ectodomain was only detected in CM of F3II-pcDNA3 cells (Figure 2A).

E-cadherin downregulation could also be associated to the expression of transcription factors that bind to the promoter region of the *CDH1* gene and repress its expression, in particular, members of the Zn-fingers, such as Snail1, and of helix-loop-helix, such as Twist1 (Foubert et al., 2010). The expression of both repressors was evaluated by PCR analysis. As shown in Figure 2B, Snail1 expression was neither detected in F3II-pcDNA3 nor in 2C1 cells. On the other side, PCR analysis revealed Twist1 expression in both cell lines (Figure 2C, left, standard PCR analysis) but higher ($P < 0.05$) in SLPI expressing cells compared with F3II-pcDNA3 cells (Figure 2C, right, qPCR analysis).

In cells that show a decrease in E-cadherin expression, an increase in the expression of N-cadherin sometimes is observed. This phenomenon, called 'cadherin switch', has been associated to a cell phenotype characterised by increased migration and invasion properties (Wheelock et al., 2008). Standard RT-PCR analysis showed presence of the N-cadherin transcript in both F3II-pcDNA3 and 2C1 cells, and a quantitative analysis using qPCR revealed a decrease ($P < 0.05$) in N-cadherin mRNA expression levels in 2C1 cells compared to F3II-pcDNA3 cells (Figure 2D). Studies run to test the expression of Placental cadherin (P-cadherin), another classical cadherin reported to have a role in the malignant phenotype of breast (Knudsen et al., 2005), showed no detectable levels of P-cadherin mRNA in F3II-pcDNA3 or 2C1 cells, under the conditions assayed (Figure 2E).

Cellular localisation of adherent complex components

The correct assembly of the components from the adherent complex allows an adequate establishment of these cellular structures and contributes to their stability and functionality. In organised epithelia, E-cadherin and β-catenin co-localise in cell–cell

Figure 2 | Decreased E-cadherin expression in SLPI-expressing 2C1 murine breast cancer cells. Assessment of possible mechanisms involved

(**A**) Detection of E-cadherin proteolysis fragments by Western immunoblotting in F3II and 2C1 total cell lysates: CTF1 = 38 kDa (left panel) and conditioned media: Ectodomain = 86 kDa (right panel). (**B** and **C**) Expression analysis of E-cadherin transcriptional repressors Snail1 (Snail, **B**) and Twist1 (Twist, **C**) mRNAs by standard RT-PCR. CN: negative control. Quantification of Twist1 expression levels (*$P < 0.05$) by means of qPCR. (**D** and **E**) Evaluation of cadherin switch: (**D**) N-cadherin mRNA expression analysis (standard and qPCR analysis) (*$P < 0.05$; right panel). (**E**) P-cadherin mRNA expression analysis (standard PCR). C+: positive control (C4HD murine mammary tumour).

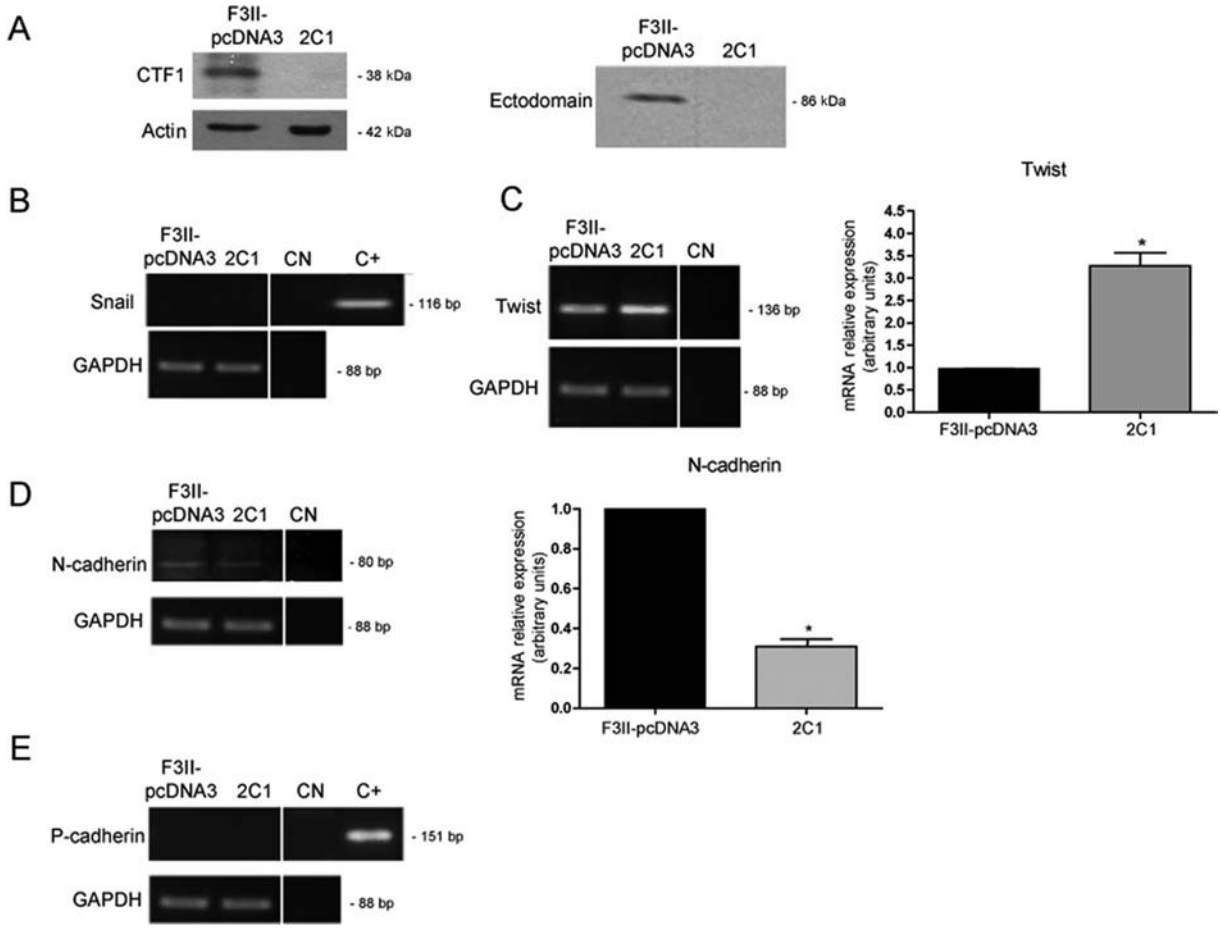

contacts and the actin cytoskeleton is organised as an adhesion belt that surrounds the inner cell side, connecting the sites of cell–cell interaction and providing strength to these associations (van Roy and Berx, 2008).

To further understand changes in E-cadherin and related proteins of the adherent complex in cells expressing SLPI, cellular localisation of E-cadherin, β-catenin and filamentous actin was evaluated in both breast tumour cells by fluorescence cytochemistry with specific antibodies to E-cadherin and β-catenin or probes to F-actin. With regard to E-cadherin, the overall percentage of cells immunoreactive to the adhesion protein was lower ($P < 0.01$) in 2C1 cells compared with control cells (2C1 = 42 ± 6% versus F3II-pcDNA3 = 94 ± 3% cells immunoreactive to E-cadherin; mean ± SEM). Evaluation of E-cadherin signal distribution (Figure 3A, right panel) also revealed differences between these cells. F3II-pcDNA3 cells depicted a typical E-cadherin membranous stain, alone or in combination with the cytoplasm, in around 30% of the cells (membrane: 6.5 ± 2.1%;

membrane + cytoplasm: 24.8 ± 0.01%); in addition, over 60% showed a signal in the cytoplasm (62.0 ± 2.8%). Contrasting, 2C1 cells showed less than 3% cells with a signal in the cell membrane without or with cytoplasm stain (membrane: 0.2 ± 0.1%; membrane + cytoplasm: 2.6 ± 1.2%, $P < 0.01$) and the remnant immunoreactive cells depicted a signal in the cytoplasm (39.4 ± 6.4%, $P < 0.01$ compared with control).

Changes in E-cadherin localisation appeared not to cause major alterations in status of actin cytoskeleton, as suggested by a similar Alexa Fluor 488-Phalloidin signal for F-actin distribution found in the two cell lines (Figure 3B).

β-catenin localisation analysis also revealed dramatic differences between F3II-pcDNA3 and 2C1 cells. In F3II-pcDNA3 cells, the adaptor protein was localised mainly in the cytoplasm without or with signal at the cell membrane (membrane + cytoplasm: 34.8 ± 1.0% cells; cytoplasm: 54.4 ± 1.4% cells) and a small proportion of cells (5.6 ± 1.2% cells) showed a β-catenin signal in the cell cytoplasm and nucleus. Contrasting, the percentage of 2C1 cells with β-catenin in the membrane + cytoplasm decreased (3.8 ± 0.4%; $P<0.001$) and in the cytoplasm and nucleus increased (cytoplasm: 69.8 ± 1% and cytoplasm + nucleus: 25.7 ± 0.5%, $P < 0.001$ compared with control) (Figure 3C). Nuclear localisation of β-catenin in 2C1 cells was confirmed in co-localisation assays with Hoechst 33342 nuclear dye (Figure 3C, right panel). These alterations in cellular localisation of the adaptor protein were not associated to changes in protein expression levels, since similar β-catenin protein levels were found in total cellular extracts of F3II-pcDNA3 and 2C1 cells evaluated by Western immunoblotting (Figure 3D).

β-Catenin and apoptosis in SLPI-expressing cells

Studies presented in the previous section were unable to show, in association to SLPI expression, changes in molecules related to downregulation of E-cadherin that could refer to a more invasive cell phenotype. Moreover, a recent report from members of this team had revealed that SLPI-expressing cells depicted signs of apoptosis (Amiano et al., 2013). Therefore, a set of studies were designed to further evaluate the occurrence of apoptosis-related molecular changes found in other cell models with nuclear localisation of β-catenin.

First, the TUNEL assay was used as a tool to detect apoptotic cells; the procedure was done in parallel to the assessment of β-catenin localisation by immunocytochemistry. In F3II-pcDNA3 cells, β-catenin was mainly localised to the cell membrane and showed no label after TUNEL staining. Contrasting 2C1 cells, that depicted a high percentage of cells with β-catenin localisation in the nucleus, had signals of apoptosis, evidenced by the fluorescent signal after TUNEL staining (Figure 4A).

The expression levels of Bcl-2 and Bax, two well-studied apoptosis-related proteins, were evaluated in 2C1 and F3II-pcDNA3 cells. As shown in Figure 4B, Bcl-2 levels were drastically reduced and the expression of the Bax protein was increased in 2C1 SLPI-expressing cells; therefore, the Bax to Bcl-2 ratio was increased ($P < 0.05$) in 2C1 cells. Moreover, levels of Bcl-xL, a 233 amino acid protein with 43% sequence identity with Bcl-2 that suppresses cell death, were decreased in the 2C1 cells compared with the F3II-pcDNA3 control cells, whereas those for Bcl-xS, a shorter variant which functions as a dominant inhibitor of Bcl-2, were similar in both cell types (Figure 4C). Altogether, these findings revealed signals of apoptosis in 2C1 SLPI-expressing breast tumour cells, which had an increased percentage of cells with nuclear β-catenin localisation.

Proteins like c-Myc and Cyclin D1 are well known as positive regulators of cell proliferation; specifically cyclins have a role in promoting cell cycle transitions via their ability to associate with and activate Cyclin-Dependent kinases (CDk), some of which (CDk2) associate with cyclins and control the G1 to S phase transition. First, c-Myc expression was found downregulated in 2C1 SLPI-expressing cells (Figure 4D). Taking into account this result and previous reports describing the ability of β-catenin to mediate growth arrest (Damalas et al., 2001), Cyclin D1 mRNA expression was evaluated, finding lower ($P < 0.05$) levels of this marker in 2C1 cells when compared with those in F3II-pcDNA3 cells (Figure 4E). Moreover, expression of the p21/WAF protein, a potent inhibitor of the cell cycle progression, was found increased ($P < 0.05$) in 2C1 cells compared with F3II-pcDNA3 cells (Figure 4F)

Figure 3 | Localisation analysis of E-cadherin, β-catenin and F-actin in SLPI-expressing 2C1 murine breast cancer cells (**A**–**C**) Fluorescent cytochemistry of (**A**) E-cadherin (**B**) F-actin and (**C**) β-catenin in F3II-pcDNA3 and 2C1 cells (scale bar: 20 μm) using specific antibodies (E-cadherin and β-catenin) or probes (F-actin, Alexa Fluor 488-Phalloidin). (**C**) Fluorescent immunocytochemistry of β-catenin coupled to nuclear staining with dye Hoechst 33342 in F3II-pcDNA3 and 2C1 cells (scale bar: 10 μm). Quantification of E-cadherin (**A**, $^{**}P < 0.01$; right panel) and β-catenin (**C**, $^{***}P < 0.001$; bottom panel) localisation in the plasma membrane, cytoplasm and nuclear compartments is also shown as indicated in the graph bar. (**D**) Western immunoblotting of β-catenin in F3II-pcDNA3 and 2C1 cells and densitometric analysis (ns: not significant).

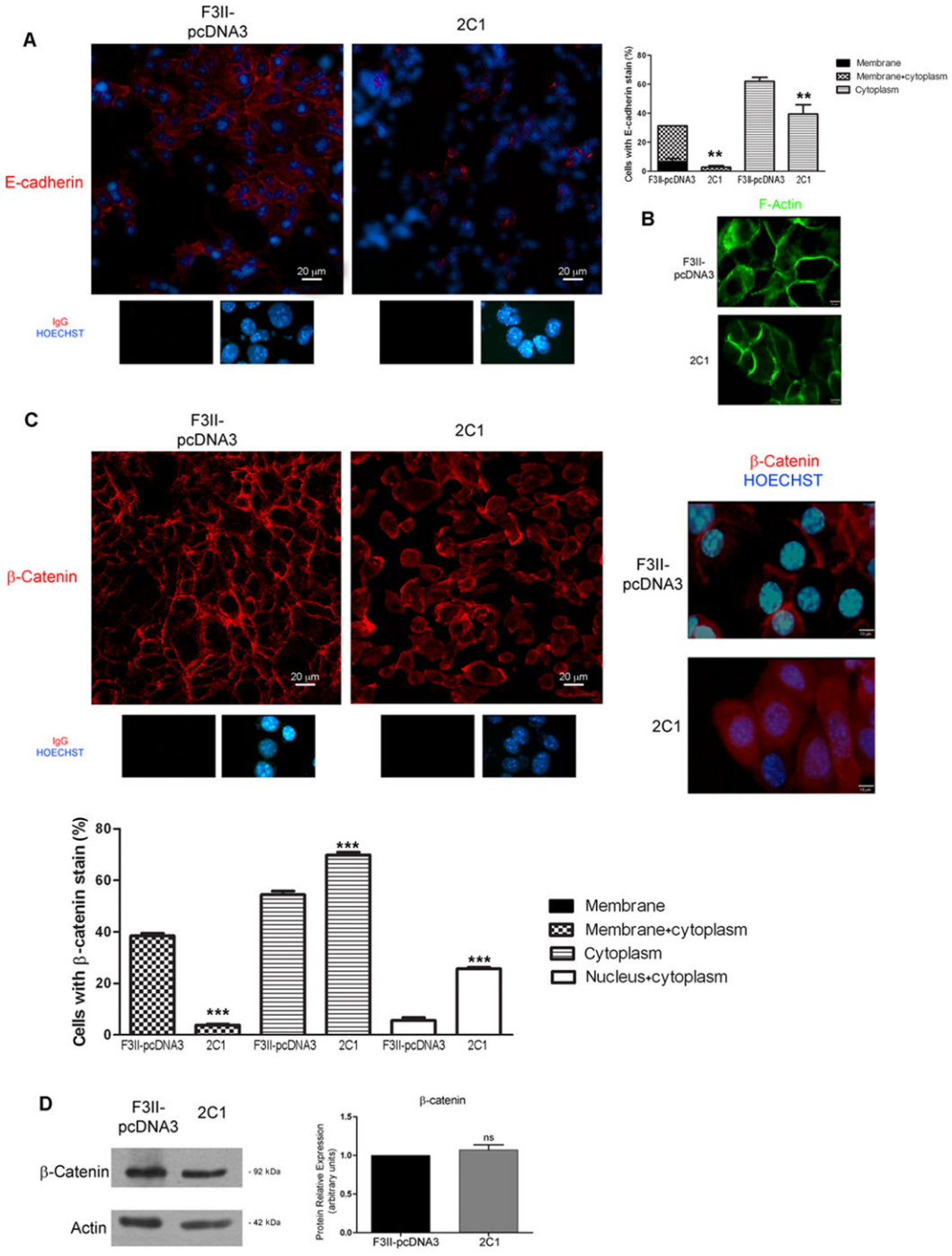

Figure 4 | β-catenin and apoptosis markers in SLPI-expressing 2C1 murine breast cancer cells

(**A**) Co-localisation analysis of β-catenin (red) and apoptotic cells (green) as determined by the TUNEL assay in 2C1 cells and in F3II-pcDNA3 control cells (three images are shown for each cell type; scale bar: 20 μm). (**B**) Western immunoblotting of Bcl-2 (left panel) and Bax (middle panel); densitometric analysis of the Bax /Bcl-2 ratio (*$P < 0.05$; right panel). (**C**) Western immunoblotting of Bcl-xL and Bcl-xS proteins (left panel), and Bcl-xS densitometry analysis (right panel). (**D**) Western immunoblotting of c-Myc (left panel) and densitometric analysis (*$P < 0.05$; right panel). (**E**) Quantitative analysis of Cyclin D1 mRNA by qPCR (*$P < 0.05$). (**F**) Western immunoblotting of p21/WAF (left panel) and densitometric analysis (*$P < 0.05$; right panel). (**G**) Quantitative analysis of Claudin-1 mRNA by qPCR (*$P < 0.05$). (**B–D**) Actin is included for total protein loading control.

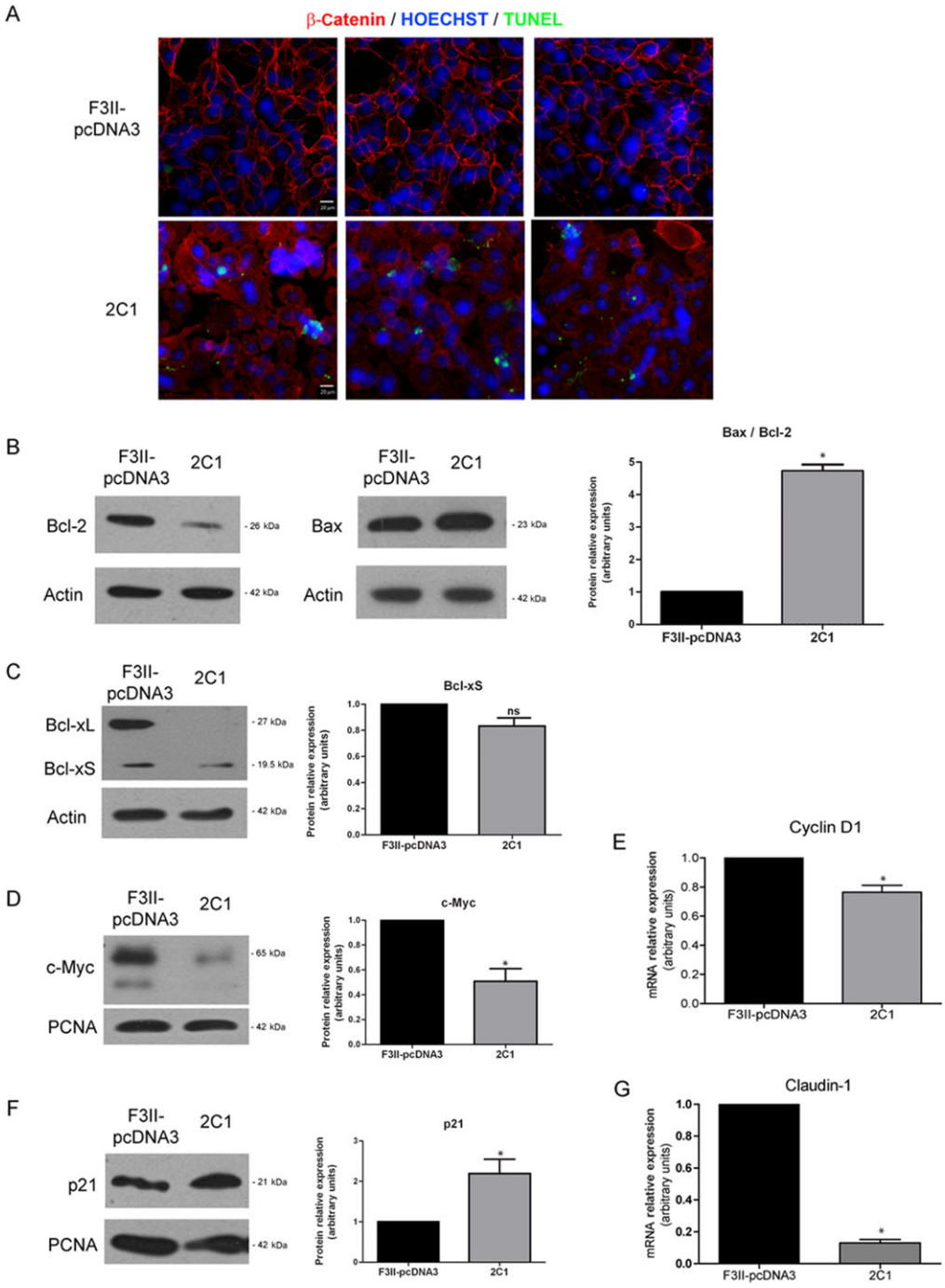

The integrity of the tight junctions has also been related to a higher resistance to apoptosis in different tumour and inflammatory models (Lee et al., 2010). Decreased ($P < 0.05$) Claudin-1 mRNA levels were found in 2C1 cells compared with controls (Figure 4G), in agreement with the higher levels of apoptosis found in 2C1 cells using different markers.

SLPI modulation of E-cadherin expression in human breast cancer cells

Based on the results obtained with the murine model, the effect of SLPI upon E-cadherin expression in a human mammary tumour cell model was evaluated. MCF-7 human breast tumour cells were stably transfected with the expression plasmid containing the coding sequence of SLPI, as indicated in *Materials and Methods*. The expression of SLPI mRNA was confirmed by standard PCR analysis in two clones selected for evaluation (5E3 and 9H6; Figure 5A, upper left panel); in agreement with these findings, a significant increase in SLPI in the CM was determined in both clones when compared with the MCF7-pcDNA3 control cells transfected with the empty plasmid (Figure 5A, upper right panel). Expression of SLPI resulted in a decrease in E-cadherin expression in both 5E3 and 9H6 clones compared with control cells, as evidenced by the lower ($P < 0.01$) level of the E-cadherin mRNA measured by qPCR (Figure 5A, lower panel).

Taking into account that SLPI is synthesised as a secretory protein, the effect of rhSLPI upon E-cadherin expression was also evaluated. MCF-7 cells were incubated with 0.4 and 4 μg/ml of rhSLPI or with vehicle (control) and the expression of E-cadherin in cell lysates was analysed by Western immunoblotting. As shown in Figure 5B, treatment of MCF-7 cells with 4 μg/ml rhSLPI lead to a decrease in E-cadherin protein levels (39 ± 6%; $P < 0.05$ compared with control; Figure 5B, right panel).

In addition to these studies, localisation of E-cadherin and β-catenin was analysed by immunofluorescence microscopy on MCF-7 treated with rhSLPI and with vehicle (control cells). With regard to E-cadherin, while most of the cells depicted a signal for the adhesion protein in both rhSLPI-treated and control cells, a decrease in signal intensity was observed in MCF-7 cells treated with rhSLPI compared to control [Figure 5C, images in left panel; signal intensity (arbitrary units) MCF7 + rhSLPI: 21 ± 2; MCF-7: 45 ± 2; $P < 0.001$]. In terms of protein distribution, treatment with rhSLPI resulted in a decreased ($P < 0.01$) percentage of cells depicting an E-cadherin signal confined to the plasma membrane (MCF7 + rhSLPI: 11 ± 1%; MCF-7: 36 ± 0.4% cells) and an increased ($P < 0.001$) proportion of cells with E-cadherin signal in the cytoplasm (MCF7 + rhSLPI: 59 ± 5%; MCF-7: 31 ± 1%) (Figure 5C). In agreement with these findings, treatment with rhSLPI was associated to a decrease ($P < 0.001$) in the amount of cells depicting β-catenin signal in the plasma membrane (MCF7 + rhSLPI: 13 ± 1%; MCF-7: 45 ± 4%), and an increase ($P < 0.001$) in those showing a staining for the adaptor protein in the cytoplasm and nucleus (MCF7 + rhSLPI: 40 ± 2%; MCF-7: 6 ± 0.1%) (Figure 5C).

Altogether, these studies revealed a decrease in E-cadherin levels and re-localisation of both E-cadherin and β-catenin in MCF-7 cells exposed to SLPI, as found in the murine mammary cell model.

Discussion

The present study was aimed at evaluating the effect of SLPI on the expression of E-cadherin and other members of the adherent complex, specifically β-catenin and F-actin, as well as on other classical cadherins and apoptosis-related proteins in cell models of breast cancer. To our knowledge, this is the first report that describes the effect of SLPI upon E-cadherin. Altogether, the study shows SLPI as a negative modulator of E-cadherin expression in murine and human models of breast cancer cells using either an experimental approach of cell cultures supplemented with the rhSLPI protein (a model that mimics cellular secreted SLPI) or, alternatively, of cells stably transfected with the sequence encoding the protease inhibitor, in which the secretion of SLPI was monitored in all cases. In experiments in which rhSLPI was supplemented to the cell culture media, the maximum protein concentration added was within the range detected in several biological fluids (*i.e.* saliva = 0.1–10 μg/ml, upper airways = 94 μg/ml and lower respiratory tract = 7 μg/ml) (Vogelmeier et al., 1991; Doumas et al., 2005). On the other side, in the model using SLPI-stable transfectants, secreted SLPI levels did not exceed values reported in biological fluids.

Figure 5 | Effect of SLPI upon E-cadherin and β-catenin expression in MCF-7 human breast cancer cells
(**A**) RT-PCR analysis of SLPI (standard; top left) and E-cadherin (qPCR; bottom) mRNA in MCF-7 cells transfected with SLPI (clones 5E3 and 9H6) (**$P < 0.01$). SLPI concentration in 5E3, 9H6 and MCF7-pcDNA3 in cell culture supernatants assessed by means of an ELISA sandwich (*$P < 0.05$) (top right). (**B**) Western immunoblotting (left panel) and densitometric analysis of E-cadherin protein levels in protein extracts from MCF-7 cells incubated with rhSLPI (right panel) (*$P < 0.05$). (**C**) Fluorescent immunocytochemistry of E-cadherin (top left) and β-catenin (bottom left) in MCF-7 cells incubated with rhSLPI; scale bar: 20 μm. Quantification of E-cadherin (**$P < 0.01$, ***$P < 0.001$; top right) and β-catenin (***$P < 0.001$; bottom right) signal in the plasma membrane, cytoplasm and nuclear compartments, is also shown, as indicated in the bar graph.

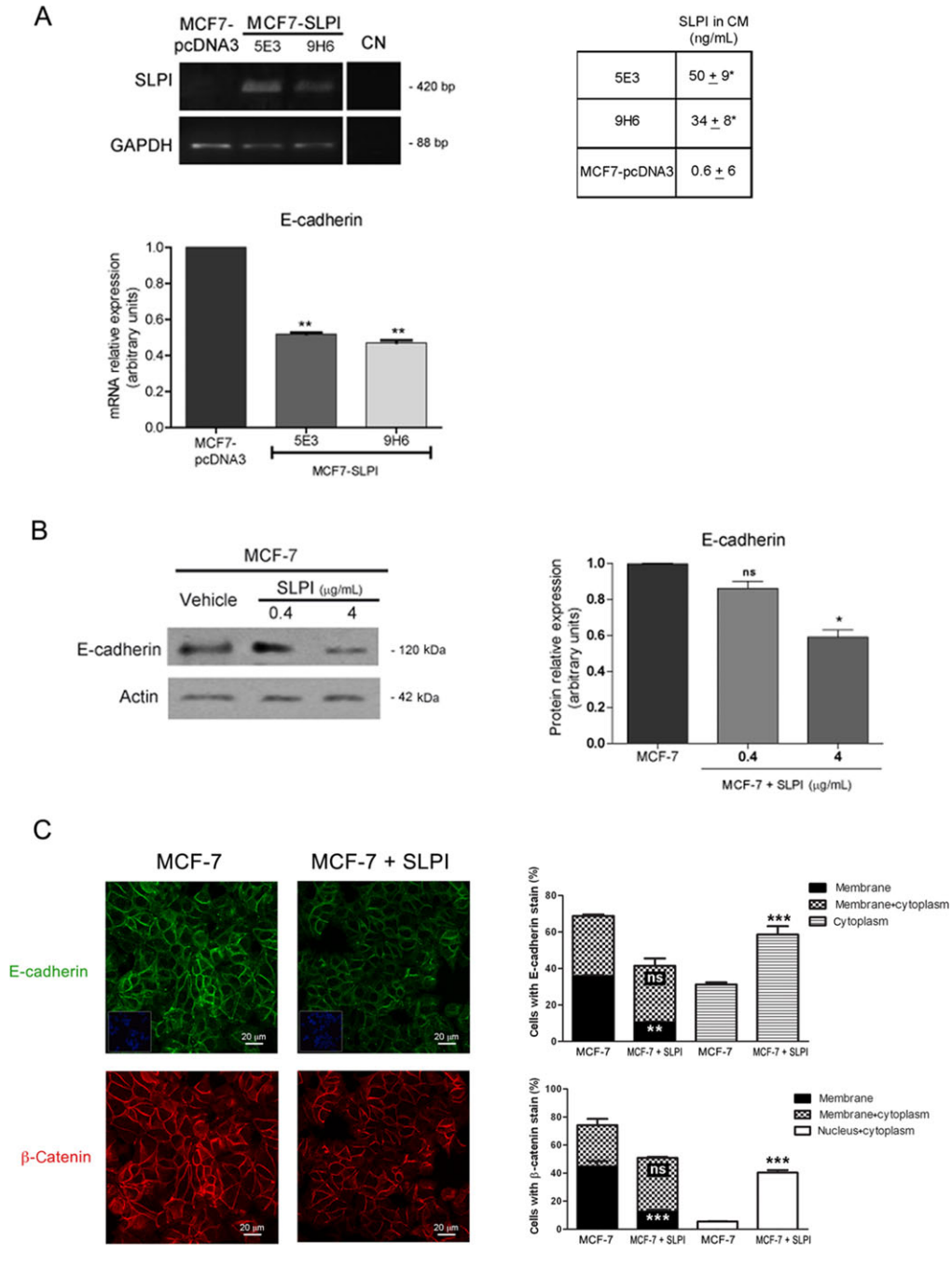

Our studies have revealed that reduced E-cadherin levels found in cells exposed to SLPI were associated with a decrease on the presence of the adhesion protein at the cell membrane and a concomitant increase in the cytoplasm. Changes in E-cadherin were also related to alterations in β-catenin cellular localisation, with re-localisation of the adaptor protein to the cell cytoplasm and nucleus. These changes were observed in both the murine and the human models. It is now well accepted that functional consequences of alterations in β-catenin expression and/or localisation during tumour progression are rather complex. Classical studies have associated an oncogenic role for nuclear β-catenin; however, more recent studies have shown in several normal and tumour cell models an association between localisation of the adaptor protein in the cell nucleus and the induction of apoptosis (Wong et al., 1998; Damalas et al., 1999; Kim et al., 2000; Peluso et al., 2000; Olmeda et al., 2003; Saegusa et al., 2004; Raab et al., 2009; Li et al., 2012; Liu et al., 2012; Lu et al., 2012; Ming et al., 2012; Zimmerman et al., 2013; Wu et al., 2014).

Changes observed in localisation of E-cadherin and β-catenin could relate to the signs of apoptosis recently reported for the 2C1 and MCF-7 cells (Amiano et al., 2013). The relationship between SLPI expression, E-cadherin, β-catenin and apoptosis was further analysed in the present investigation using the murine model, since 2C1 cells expressing SLPI were found not to develop tumours when injected in BALB/c mice (Amiano et al., 2011). Our results showing higher signs of apoptosis in SLPI expressing cells revealed by the TUNEL assay are also in line with previous findings from us reporting higher levels of Annexin-V and caspase-3 positive cells among 2C1 cells (Amiano et al., 2013) as well as with studies published in other cell models (Nakamura et al., 2008). Specifically regarding β-catenin and apoptosis, findings from TUNEL and β-catenin staining are in agreement with a previous study using the same experimental approach that reported a TUNEL positive signal in cells mainly depicting β-catenin nuclear localisation (Kim et al., 2000).

To explore additional molecules involved in apoptosis, cell proliferation and cell cycle arrest, studies were carried out to evaluate expression of Bax/Bcl-2 ratio (as well as Bcl-xL and Bcl-xS), c-Myc, cyclin D1 and p21. Results obtained on c-Myc expression in 2C1 cells are in line with a recent report that shows that downregulation of c-Myc triggers apoptosis through an increase of Bax and a decrease of Bcl-2 levels concomitant with caspase-3 activation (Russo et al., 2003), a group of changes that have been observed in this and in a previous report (Amiano et al., 2013), and are in agreement with a previous report showing β-catenin mediated enzastaurin-induced growth arrest in multiple myeloma cell cultures (Raab et al., 2009).

The integrity of the tight junctions has also been related to a higher resistance to apoptosis in different tumour and inflammatory models (Lee et al., 2010). In particular, downregulation of Claudin-1 in breast tumour cells has been associated to a higher sensitivity to apoptotic-inducing agents (Akasaka et al., 2010) and a recent study has pointed out its relationship with apoptosis induced by β-catenin (Liu et al., 2012). Moreover, a recent report has shown that MCF-7 cells treated with Claudin-1siRNA were found to have decreased levels of Cyclin D1 (Liu et al., 2012), results that agree with findings from this study. In line with these results, 2C1 cells treated with SLPI-siRNA restored Claudin-1 mRNA levels to normal (data not shown). Altogether, these findings lead us to propose a relationship between a decrease in E-cadherin in association to SLPI expression, β-catenin nuclear localisation as result of disruption of the adherent complex, and changes in gene expression towards apoptosis and cell cycle arrest in the murine mammary tumour cell model.

The findings in the animal cell model prompted us to evaluate the effect of SLPI upon E-cadherin expression and localisation in a human model. Results with MCF-7 stably transfected or treated with exogenous rhSLPI revealed the SLPI negative effect on E-cadherin expression that resulted in re-localisation of E-cadherin to the cell cytoplasm and β-catenin to the cell nucleus. In agreement with these results, a similar E-cadherin and β-catenin cellular re-localisation has been recently reported in MCF-7 breast tumour cells in response to the pro-apoptotic cytokine TNF-α (Liu et al., 2012).

In conclusion, the studies here presented describe, for the first time, changes in E-cadherin and β-catenin in breast tumour cells in association to the expression of SLPI. Taken together, SLPI expression in breast tumour cells resulted in the disruption of the E-cadherin/β-catenin complex and altered homeostasis of proteins controlling the apoptotic process and cell

cycle progression, resulting in activation of apoptosis and cell cycle arrest molecular related events. The implications of the β-catenin mediated pro-apototic effect of SLPI may contribute to future decisions in putative novel treatments in breast cancer, taking into account the potential use of SLPI in the therapeutics of this disease and the impact of changes in the adherent complex and tumour progression in breast cancer, a pathology that still remains as the most common cancer in women and the main cause of deaths due to cancer in women worldwide.

Materials and methods

Chemicals

Chemicals were of analytical and tissue culture grade. The following antibodies were used: a monoclonal antibody towards E-cadherin cytoplasmic domain (610181, BD Biosciences, San Diego, CA, USA) and polyclonal antibody towards E-cadherin extracellular domain [H-108, Santa Cruz Biotechnology (SCB), Santa Cruz, CA, USA]; anti β-catenin (610153; BD); anti Bcl-2 (N-19; SCB); anti Bax (N-20, polyclonal; SCB); anti Bcl-$x_{S/L}$ (S-18, polyclonal; SCB); anti c-Myc (D84C12, monoclonal; Cell Signaling, Danvers, MA, USA); anti p21 (C-19, polyclonal; SCB); anti actin (I-19; SCB); anti PCNA (PC10, monoclonal; SCB). For immunocytochemistry protocols, Cy3-labelled anti-mouse (Sigma, San Luis, MO, USA) IgGs were used as secondary antibody. Anti-mouse (Vector Lab. Inc., Burlingame, CA, USA), anti-rabbit or anti-goat IgGs coupled to horseradish peroxidase were used as secondary antibodies in Western immunoblotting procedures. In control experiments, primary antibodies were replaced by purified mouse, rabbit or goat IgGs, as required.

rhSPLI was expressed in bacteria and purified as previously reported (Amiano et al., 2011). Before using rhSLPI, potential lipopolysaccharide (LPS) contaminant was removed with a polymyxin B column (Sigma); presence of remaining LPS was evaluated using the Lymulus test (Cambrex, Walkersville, MD, USA).

Cell lines

Mouse (F3II) and human (MCF-7) breast cancer cells were selected as models to treat with rhSLPI or to generate stable transfectants expressing the protease inhibitor. The murine F3II is a hormone-independent mammary carcinoma cell line derived from BALB/c mice, as previously described (Alonso et al., 1996), and has been extensively characterised in terms of its invasive properties (Alonso et al., 1996; Ladeda et al., 1998; Menna et al., 2003). The MCF-7 (HTB-22™; American Type Culture Collection, ATCC, Manassas, VA, USA) cell line is a worldwide well studied hormone-dependent human breast cancer cell line derived from a pleural effusion of a 69-y.o. caucasian woman diagnosed with an invasive breast ductal carcinoma.

In experiments shown in Figure 1A and 5C, F3II and MCF-7 cells were treated with exogenous rhSLPI (see below).

Stable transfectants of SLPI for both F3II and MCF-7 cell lines used in this study were obtained as recently detailed (Amiano et al., 2013). Basically, F3II-SLPI (clone 2C1) and MCF7-SLPI (clones 5E3 and 9H6) cells were generated by transfecting cells with a pcDNA3 plasmid containing the hSLPI cDNA using standard procedures with Lipofectamin™ (Thermo-Life, Carlsbad, CA, USA). F3II and MCF-7 cells transfected with the empty plasmid (MCF7-pcDNA3 and F3II-pcDNA3, respectively) served as control.

All cell lines (parental and transfectants) were cultured in RPMI 1640 (GIBCO, Thermo-Life) culture medium supplemented with 10% foetal bovine serum, 2 mM L-glutamine and 40 μg/ml gentamycin at 37°C in an atmosphere of 5% of CO_2 in air up to 50–80% confluence, depending on the experimental design. Low-passage cell lines were used; in addition, quality-control tests were done by monitoring cellular morphology and cell growth rates as well as mycoplasma detection with Hoechst 33258 (Sigma). All experiments were run in triplicates.

Cell treatment with rhSLPI

F3II and MCF-7 cells were incubated for 48 h with rhSLPI (0.04–4 μg/ml) or vehicle (control condition) (Amiano et al., 2013). At the end of the incubation, total protein extracts were prepared and E-cadherin expression was analysed by SDS-PAGE followed by Western immunoblotting with specific antibodies (Lapyckyj et al., 2010). In experimental protocols of cell treatment with SLPI, MCF-7 cells were grown in Lab-Tek® chamber slides (Nunc-Nalge, Penfield, NY, USA), treated with 4 μg/ml SLPI or vehicle under the same conditions, harvested, fixed and subjected to immunofluorescence microscopy analysis.

ELISA evaluation of SLPI levels

SLPI concentration was measured in cell culture supernatants of human and murine stable transfectants by means of ELISA sandwich assay, using a mAb anti-hSLPI (Clone 20409; R&D Systems, Minneapolis, MN, USA), a rabbit polyclonal antibody (HyCult Biotechnology, Uden, The Netherlands) and a goat polyclonal anti-rabbit IgG conjugated with peroxidase (Chemicon, Billerica, MA, USA). All samples were run in triplicates (Amiano et al., 2013).

Preparation of small Interfering RNA against hSLPI and cell treatment

A SLPI small interfering RNA duplex (siSLPI) was synthesised by Thermo-Life Technologies (Thermo-Life) and added to the 2C1 murine breast tumour cells over-expressing SLPI as recently reported (Amiano et al., 2013).

Protein extraction, SDS-PAGE and Western immunoblotting protocols

Total protein extracts were prepared from F3II and MCF-7 cells treated with rhSLPI or vehicle, as well as from F3II-pcDNA3 and 2C1 stable transfectants, and subjected to SDS-PAGE followed by Western immunoblotting procedures (Lapyckyj et al., 2010). Protein immunodetection was done using primary antibodies against E-cadherin, β-catenin, actin, PCNA, p21, c-Myc, Bax, Bcl-$x_{S/L}$ and Bcl-2 using standard procedures. In all cases, immunodetection was specific, since no signal was obtained when the primary antibody was replaced by the corresponding normal IgG at the same concentration (data not shown).

Immunocytochemical analysis

Cells grown on glass coverslips (80% confluence) or Lab-Tek® chamber slides were fixed with 4% paraformaldehyde in PBS

Table 1 | Primer sequences and amplicon sizes for PCR fragments shown in the report

Primer (species) (amplicon size, # bp)	Forward	Reverse
SLPI (human) (420 bp)	GGCAGGAATCAAGCTTTCACA	TCACCATGAAGTCCAGCGGC
E-cadherin (murine) (100 bp)	GCTCTCATCATCGCCACAG	CTGGGATGGGAGCGTTGTC
Snail1 (murine) (111 bp)	CACGCTGCCTTGTGTCTG	CAGTGGGTGCAGGAGAATGG
Twist1 (murine) (136 bp)	GCTATGTGGCCCACGAGC	GAAACAATGACATCTAGGTCTCCG
N-cadherin (murine) (79 bp)	GCCATCATCGCTATCCTTC	CCCGCCGTTTCATCCATCC
P-cadherin (murine) (151 bp)	CGGGAACTTCATCATCGAGAACCTG	CTGATCCTGGTCGGAGGCGG
Cyclin D1 (murine) (105 bp)	CGCCCTCCGTATCTTACT	CGCACTTCTGCTCCTCAC
Claudin-1 (murine) (162 bp)	TCGTGACCGCTCAGGCCATC	CGATCAGCCCCAGCAGGATGC
GAPDH (murine) (87 bp)	TGCACCACCAACTGCTTAGC	GGCATGGACTGTGGTCATGAG
β-Actin (murine) (93 bp)	CAGCCTTCCTTCTTGGG	GAGGTCTTTACGGATGTCA

for 10 min, and subjected to immunocytochemistry to assess E-cadherin and β-catenin localisation (Lapyckyj et al., 2010). In negative controls, immunodetection protocol was followed by nuclear cell staining with Hoechst 33342 (Sigma). In experiments shown in Figure 4A, immunocytochemistry for β-catenin was followed by nuclear staining or by TUNEL staining (see below). Filamentous actin (F-actin) distribution was assessed with Alexa Fluor 488-Phalloidin (Thermo-Life). Stained cells were observed in a Nikon confocal fluorescence microscope coupled to an image analyser (LSM Image Browser, Nikon, Japan). To quantify the% of cells immunoreactive for E-cadherin or β-catenin and protein subcellular distribution (cell membrane, cytoplasm and nucleus), images were analysed with the Image-J program (NIH, USA); at least triplicates of 200 cells were evaluated in each case.

TUNEL assay

TUNEL assay was performed with the In situ Cell Death Detection Kit, Fluorescein (Roche Diagnostics Corp., Indianapolis, IN, USA). TUNEL reaction was carried out for 60 min at 37°C and samples were analysed in a confocal fluorescent microscope.

RNA extraction and RT-PCR procedures

Total RNA was isolated with the TRIzol™ reagent (Life) and synthesis of complementary DNA (cDNA) was performed with oligo-dT and SuperScript™ III Reverse Transcriptase (Thermo-Life). Negative controls (omitting RNA or reverse transcriptase) were included in all cases (Lapyckyj et al., 2010). Reverse transcription procedures were verified by amplification of a fragment for the GlycerAldehyde 3-Phosphate DeHydrogenase (GAPDH) in human and mouse cells. Standard end point PCR amplification protocols were carried out using *Taq*I DNA polymerase (Thermo-Life). Primers for cDNA amplification and amplification fragments expected sizes for human SLPI, human and murine E-cadherin and GAPDH mRNA, as well as for murine Snail1, Twist1, N-cadherin, P-cadherin, Cyclin D1, Claudin-1 and β-actin are listed (see Table 1) or have been previously published (Lapyckyj et al., 2010).

A quantitative assessment of mRNA levels was done using real time PCR (qPCR) with the Applied Biosystems 7500 Real Time PCR unit and the SYBR Green® PCR Master Mix (Thermo-Life). All samples were run in triplicates and negative controls (no template) were included in all cases. To confirm specificity of the signal, melting curves were done in each run. Relative expression was calculated using β-actin (murine) or GAPDH (human) as endogenous control and control cells as reference. The calculation describing these relations is $2^{-\Delta\Delta Ct}$, where $\Delta\Delta Ct = [\Delta Ct$ test sample $- \Delta Ct$ reference sample], and $\Delta Ct = [Ct$ gene under study $-$ Ct endogenous gene] (Lapyckyj et al., 2010).

Statistical analysis

All experiments were run in triplicates. Statistical analyses were performed using GraphPad Prism 5.01 (GraphPad Software, San Diego, CA, USA). Data are presented as the mean ± Standard Error of the Mean (SEM). Analyses done on SLPI and control stable transfectants (murine: 2C1 and F3II-pcDNA3 clones; human: 5E3, 9H6 and MCF7-pcDNA3 clones) were done using Mann–Whitney test, whereas evaluations of F3II or MCF-7 cells treated with exogenous rhSLPI or vehicle were done with Wilcoxon signed-ranked test. Analyses of more than two groups were done using ANOVA followed by Bonferroni or Dunn's comparison test. A $P < 0.05$ was considered significant for each comparison.

Authors contribution

M.R. and L.L. (equal contribution) performed data acquisition, analysis and/or interpretation and in drafting the manuscript. N.A. participated in preparation of materials for the experimental design, as well as in performing data acquisition and interpretation. M.J.B. participated in data acquisition, analysis and interpretation. M.S. participated in preparation of some materials for the experimental design. E.C. participated in the conception of the study as well as in elaborating the manuscript. M.H. V.-L., corresponding author, was involved in the conception and design of the study, in the data analysis and/or interpretation, as well as drafting and elaborating the manuscript and the revised version. All authors have participated sufficiently in the work to take public

responsibility for appropriate portions of the content, and gave final approval of the published version.

Acknowledgements

Authors are very grateful to Dr. D. Alonso (University of Quilmes, Buenos Aires, Argentina) who provided us the F3II murine hormone-independent mammary carcinoma cell line derived from BALB/c, as well as to Dr. R.I. Barañao and M. Tessone (IBYME), to Dr. A. Schinder (Leloir Institute, Buenos Aires, Argentina) for providing us some tools to perform these studies and to Dr. P. Pomata (IBYME) for his help with the confocal microscopy analyses.

Funding

This project has been supported by grants from the Agencia Nacional de Promoción Científica y Tecnológica (ANPCyT, PICT5–26110 and PICT-SU 1072) and from CONICET (PIP-2120) to M.H.V.L. and from ANPCYT (PICT 2331) to E.C.

Conflict of interest statement

The authors have declared no conflict of interest.

References

Akasaka, H., Sato, F., Morohashi, S., Wu, Y., Liu, Y., Kondo, J., Odagiri, H., Hakamada, K. and Kijima, H. (2010) Anti-apoptotic effect of claudin-1 in tamoxifen-treated human breast cancer MCF-7 cells. BMC Cancer **10**, 548

Alonso, D.F., Farías, E.F., Urtreger, A., Ladeda, V., Vidal, M.C. and Bal De Kier Joffé, E. (1996) Characterization of F3II, a sarcomatoid mammary carcinoma cell line originated from a clonal subpopulation of a mouse adenocarcinoma. J. Surg. Oncol. **62**, 288–297

Amiano, N.O., Costa, M.J., Reiteri, R.M., Payes, C., Guerrieri, D., Tateosian, N.L., Sanchez, M.L., Maffia, P.C., Diament, M., Karas, R., Orqueda, A., Rizzo, M., Alaniz, L., Mazzolini, G., Klein, S., Sallenave, J.M. and Chuluyan, H.E. (2013) Anti-tumor effect of SLPI on mammary but not colon tumor growth. J. Cell Physiol. **228**, 469–475

Amiano, N., Reiteri, R.M., Costa, M.J., Tateosian, N. and Chuluyan, H.E. (2011) Immunotherapy with SLPI over-expressing mammary tumor cells decreases tumor growth. Cancer Immunol. Immunother. **60**, 895–900

Angst, B.D., Marcozzi, C. and Magee, A.I. (2001) The cadherin superfamily. J. Cell Sci. **114**, 625–626

Birchmeier, W., Hulsken, J. and Behrens, J. (1995) E-cadherin as an invasion suppressor. Ciba Found. Symp. **189**, 124–136

Cimino, D., Fuso, L., Sfiligoi, C., Biglia, N., Ponzone, R., Maggiorotto, F., Russo, G., Cicatiello, L., Weisz, A., Taverna, D., Sismondi, P. and De Bortoli, M. (2008) Identification of new genes associated with breast cancer progression by gene expression analysis of predefined sets of neoplastic tissues. Int. J. Cancer **123**, 1327–1338

Conacci-Sorrell, M., Zhurinsky, J. and Ben Ze'ev, A. (2002) The cadherin-catenin adhesion system in signaling and cancer. J. Clin. Invest. **109**, 987–991

Damalas, A., Ben-Ze'ev, A., Simcha, I., Shtutman, M., Leal, J.F., Zhurinsky, J., Geiger, B. and Oren, M. (1999) Excess beta-catenin promotes accumulation of transcriptionally active p53. EMBO J. **18**, 3054–3063

Damalas, A., Kahan, S., Shtutman, M., Ben-Ze'ev, A. and Oren, M. (2001) Deregulated beta-catenin induces a p53- and ARF-dependent growth arrest and cooperates with Ras in transformation. EMBO J. **20**, 4912–4922

Day, M.L., Zhao, X., Vallorosi, C.J., Putzi, M., Powell, C.T., Lin, C. and Day, K.C. (1999) E-cadherin mediates aggregation-dependent survival of prostate and mammary epithelial cells through the retinoblastoma cell cycle control pathway. J. Biol. Chem. **274**, 9656–9664

Doumas, S., Kolokotronis, A. and Stefanopoulos, P. (2005) Anti-inflammatory and antimicrobial roles of secretory leukocyte protease inhibitor. Infect. Immun. **73**, 1271–1274

Foubert, E., De Craene, B. and Berx, G. (2010) Key signalling nodes in mammary gland development and cancer. The Snail1-Twist1 conspiracy in malignant breast cancer progression. Breast Cancer Res. **12**, 206

Hu, Y., Sun, H., Drake, J., Kittrell, F., Abba, M.C., Deng, L., Gaddis, S., Sahin, A., Baggerly, K., Medina, D. and Aldaz, C.M. (2004) From mice to humans: identification of commonly deregulated genes in mammary cancer via comparative SAGE studies. Cancer Res. **64**, 7748–7755

Kim, K., Pang, K.M., Evans, M. and Hay, E.D. (2000) Overexpression of beta-catenin induces apoptosis independent of its transactivation function with LEF-1 or the involvement of major G1 cell cycle regulators. Mol. Biol. Cell **11**, 3509–3523

Kluger, H.M., Kluger, Y., Gilmore-Hebert, M., DiVito, K., Chang, J.T., Rodov, S., Mironenko, O., Kacinski, B.M., Perkins, A.S. and Sapi, E. (2004) cDNA microarray analysis of invasive and tumorigenic phenotypes in a breast cancer model. Lab. Invest. **84**, 320–331

Knudsen, K.A. and Wheelock, M.J. (2005) Cadherins and the mammary gland. J. Cell Biochem. **95**, 488–496

Ladeda, V., Aguirre Ghiso, J.A. and Bal de Kier Joffé, E. (1998) Function and expression of CD44 during spreading, migration, and invasion of murine carcinoma cells. Exp. Cell Res. **242**, 515–527

Lapyckyj, L., Castillo, L.F., Matos, M.L., Gabrielli, N.M., Luthy, I.A. and Vazquez-Levin, M.H. (2010) Expression analysis of epithelial cadherin and related proteins in IBH-6 and IBH-4 human breast cancer cell lines. J. Cell Physiol. **222**, 596–605

Lee, J.W., Hsiao, W.T., Chen, H.Y., Hsu, L.P., Chen, P.R., Lin, M.D., Chiu, S.J., Shih, W.L. and Hsu, Y.C. (2010) Upregulated claudin-1 expression confers resistance to cell death of nasopharyngeal carcinoma cells. Int. J. Cancer **126**, 1353–1366

Li, W., Tong, H., Huang, X., Wang, W., Wu, H. and Lin, S. (2012) High levels of β-catenin promote IFNγ-induced apoptosis in hepatocellular carcinoma cells. Oncol. Lett. **4**, 1092–1096

Liu, Y., Wang, L., Lin, X.Y., Wang, J., Yu, J.H., Miao, Y. and Wang, E.H. (2012) Anti-apoptotic effect of claudin-1 on TNF-alpha-induced apoptosis in human breast cancer MCF-7 cells. Tumour Biol. **33**, 2307–2315

Lu, W., Jia, G., Meng, X., Zhao, C., Zhang, L., Ren, Y., Pan, H. and Ni, Y. (2012) Beta-catenin mediates the apoptosis induction effect of celastrol in HT29 cells. Life Sci. **91**, 279–283

Menna, P.L., Skilton, G., Leskow, F.C., Alonso, D.F., Gomez, D.E. and Kazanietz, M.G. (2003) Inhibition of aggressiveness of metastatic mouse mammary carcinoma cells by the beta2-chimaerin GAP domain. Cancer Res. **63**, 2284–2291

Ming, M., Wang, S., Wu, W., Senyuk, V., Le Beau, M.M., Nucifora, G. and Qian, Z. (2012) Activation of Wnt/β-catenin protein signaling

induces mitochondria-mediated apoptosis in hematopoietic progenitor cells. J. Biol. Chem. **287**, 22683–22690
Nakamura, K., Takamoto, N., Hongo, A., Kodama, J., Abrzua, F., Nasu, Y., Kumon, H. and Hiramatsu, Y. (2008) Secretory leukoprotease inhibitor inhibits cell growth through apoptotic pathway on ovarian cancer. Oncol. Rep. **19**, 1085–1091
Olmeda, D., Castel, S., Vilaro, S. and Cano, A. (2003) Beta-catenin regulation during the cell cycle: implications in G2/M and apoptosis. Mol. Biol. Cell **14**, 2844–2860
Peluso, J.J., Pappalardo, A. and Hess, S.A. (2000) Effect of disrupting cell contact on the nuclear accumulation of beta-catenin and subsequent apoptosis of rat ovarian surface epithelial cells in vitro. Endocrine **12**, 295–302
Raab, M.S., Breitkreutz, I., Tonon, G., Zhang, J., Hayden, P.J., Nguyen, T., Fruehauf, J.H., Lin, B.K., Chauhan, D., Hideshima, T., Munshi, N.C., Anderson, K.C. and Podar, K. (2009) Targeting PKC: a novel role for beta-catenin in ER stress and apoptotic signaling. Blood **113**, 1513–1521
Russo, P., Arzani, D., Trombino, S. and Falugi, C. (2003) C-myc down-regulation induces apoptosis in human cancer cell lines exposed to RPR-115135 (C31H29NO4), a non-peptidomimetic farnesyltransferase inhibitor. J. Pharmacol. Exp. Ther. **304**, 37–47
Saegusa, M., Hashimura, M., Kuwata, T., Hamano, M. and Okayasu, I. (2004) Beta-catenin simultaneously induces activation of the p53-p21WAF1 pathway and overexpression of cyclin D1 during squamous differentiation of endometrial carcinoma cells. Am. J. Pathol. **164**, 1739–1749
Takeichi, M. (1977) Functional correlation between cell adhesive properties and some cell surface proteins. J. Cell Biol. **75**, 464–474
van Roy, F. and Berx, G. (2008) The cell-cell adhesion molecule E-cadherin. Cell Mol. Life Sci. **65**, 3756–3788
Vogelmeier, C., Hubbard, R.C., Fells, G.A., Schnebli, H.P., Thompson, R.C., Fritz, H. and Crystal, R.G. (1991) Anti-neutrophil elastase defense of the normal human respiratory epithelial surface provided by the secretory leukoprotease inhibitor. J. Clin. Invest. **87**, 482–488
Wang, L., Li, Z., Wang, C., Yang, Y., Sun, L., Yao, W., Cai, X., Wu, G., Zhou, F. and Zha, X. (2009) E-cadherin decreased human breast cancer cells sensitivity to staurosporine by up-regulating Bcl-2 expression. Arch. Biochem. Biophys. **481**, 116–122
Wheelock, M.J., Shintani, Y., Maeda, M., Fukumoto, Y. and Johnson, K.R. (2008) Cadherin switching. J. Cell Sci. **121**, 727–735
Wong, M.H., Rubinfeld, B. and Gordon, J.I. (1998) Effects of forced expression of an NH2-terminal truncated beta-Catenin on mouse intestinal epithelial homeostasis. J. Cell Biol. **141**, 765–777
Wu, X., Deng, G., Hao, X., Li, Y., Zeng, J., Ma, C., He, Y., Liu, X. and Wang, Y. (2014) A caspase-dependent pathway is involved in Wnt/β-catenin signaling promoted apoptosis in Bacillus Calmette-Guerin infected RAW264.7 macrophages. Int. J. Mol. Sci. **15**, 5045–5062
Zimmerman, Z.F., Kulikauskas, R.M., Bomsztyk, K., Moon, R.T. and Chien, A.J. (2013) Activation of Wnt/β-catenin signaling increases apoptosis in melanoma cells treated with trail. PLoS One **8**, e69593

Received: 9 November 2013; Accepted: 1 July 2014; Accepted article online: 8 July 2014

